

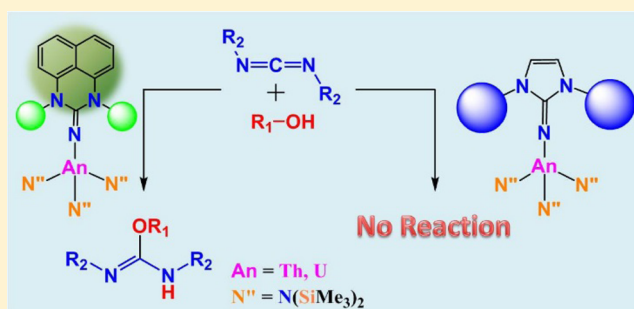
Actinide Complexes Possessing Six-Membered N-Heterocyclic Iminato Moieties: Synthesis and Reactivity

Tapas Ghatak, Natalia Fridman, and Moris S. Eisen*^{1b}

Schulich Faculty of Chemistry, Technion – Israel Institute of Technology, Haifa City, 32000, Israel

Supporting Information

ABSTRACT: A novel class of ligand systems possessing a six-membered N-heterocyclic iminato [perimidin-2-iminato ($\text{Pr}^{\text{R}}\text{N}$, where R = isopropyl, cycloheptyl)] moiety is introduced. The complexation of these ligands with early actinides ($\text{An} = \text{Th}$ and U) results in powerful catalysts [$(\text{Pr}^{\text{R}}\text{N})\text{An}(\text{N}(\text{SiMe}_3)_2)_3$] (3–6) for exigent insertion of alcohols into carbodiimides to produce the corresponding isoureas in short reaction times with excellent yields. Experimental, thermodynamic, and kinetic data as well as the results of stoichiometric reactions provide cumulative evidence that supports a plausible mechanism for the reaction.



The rapid growth in the field of organometallic and coordination chemistry concerning early actinide compounds (thorium and uranium) has been the subject of intense investigation over the past three decades that has achieved a high level of research elegance.¹ These compounds have drawn special attention due to their remarkable performances in catalytic transformations because of their unique structure–reactivity relationships.² The state of the art in particular includes a large variety of actinide-mediated carbon heteroatom bond formations, which are generally achieved by the hydroelementation of unsaturated bonds such as the hydroamination,³ hydrothiolation,⁴ hydrosilylation,⁵ etc. These types of catalytic processes are of interest since they are involved in an atom-economical route for the synthesis of various families of organic molecules.⁶ However, taking into consideration the high oxophilicity of the actinides, which results in strong $\text{An}-\text{O}$ bond strength ($\text{Th}-\text{O} = 208.0$ kcal/mol, $\text{U}-\text{O} = 181.0$ kcal/mol),⁷ catalytic transformations with oxygen containing substrates remain a major challenge. A limited number of catalytic transformations involving oxygen-containing substrates have been reported, such as the catalytic dimerization of aldehydes to esters promoted by actinide complexes bearing the Cp^* ($\text{Cp}^* = \text{C}_5\text{Me}_5$) or the isolobal imidazolin-2-iminato ligands ($\text{Im}^{\text{R}}\text{N}$, where $\text{R} = \text{tBu}, \text{Dipp}, \text{Mes}$),⁸ the ring-opening polymerization of lactones catalyzed by $\text{Cp}^*_2\text{Th}(\text{Im}^{\text{R}}\text{N})(\text{Me})$ ⁹ and $[\text{UO}_2(\text{OAr})_2(\text{THF})_2]$,¹⁰ and the ring-opening polymerization of propylene oxide and cyclohexene oxide mediated by uranyl aryloxide, $[\text{UO}_2(\text{OAr})_2(\text{THF})_2]$, uranyl chloride $[\text{UO}_2\text{Cl}_2(\text{THF})_3]$ or $[\text{UO}_2\text{Cl}_2(\text{THF})_2]$ as precatalyst.¹¹ However, the most remarkable example has been the intramolecular hydroalkoxylation/cyclization of alkynyl alcohols affording cyclic ethers mediated by the constrained geometry catalysts $(\text{CGC})\text{Th}(\text{NMe}_2)_2$.^{4a} This latter reaction was long thought to be unrealistic due to the potential formation of intractable actinide-oxo species.

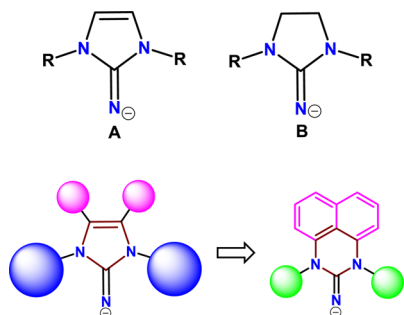
An alternative method for the formation of the carbon–heteroatom bonds is the insertion of $\text{E}-\text{H}$ ($\text{E} = \text{N}, \text{O}, \text{P}, \text{S}$) into various heterocumulenes, affording guanidine, isoureas, phosphaguanidine, and thiourea products, with great potential applications in coordination,¹² and medicinal chemistry.¹³

In a recent report, we disclose that, although the imidazolin-2-iminato complexes, $[(\text{Im}^{\text{R}}\text{N})\text{An}\{(\text{N}(\text{SiMe}_3)_2)_3\}]$ ($\text{An} = \text{Th}, \text{U}$), are excellent catalysts for the insertion of nonoxygenated species into various heterocumulenes, the challenging insertion of oxygenated substances into carbodiimides remained infeasible.^{14,15} We have recently disclosed that highly constrained and sterically opened actinide metallacycles $[\{(\text{Me}_3\text{Si})_2\text{N}\}_2\text{An}\{\kappa^2\text{-C}, \text{N}-\text{CH}_2\text{Si}(\text{CH}_3)_2\text{N}(\text{SiMe}_3)_2\}]$ ($\text{An} = \text{Th}$ (1), U (2)) can be utilized as efficient precatalysts for the exigent insertion, for actinides, of alcohols into carbodiimides.¹⁶ The difference of the aforementioned two actinide systems is the presence of a highly steric encumbered imidazolin-2-iminato ligand, which hindered the substrates to come in close proximity with the active center. Inspired by this finding, we sought to design a new family of highly nucleophilic ligands, which are isolobal with imidazolin-2-iminato or cyclopentadienyl moieties.¹⁷ The N-heterocyclic iminato species have been restricted to the five-membered heterocyclic rings, whereas **A** and **B** represent the leading architectures of this type of ligands (Scheme 1).

Strategic modification of these core structures can be achieved by three methods: (1) change in wingtip substitutions, (2) modification of backbone, and (3) expansion of ring size. Hence, we sought to design N-heterocyclic imine moieties around a unique perimidine core, in order that all

Received: January 15, 2017

Scheme 1. Schematic Presentation of the Imidazolin-2-iminato (A), the Imidazolidin-2-iminato (B), and the Perimidin-2-iminato Core (Bottom) Systems



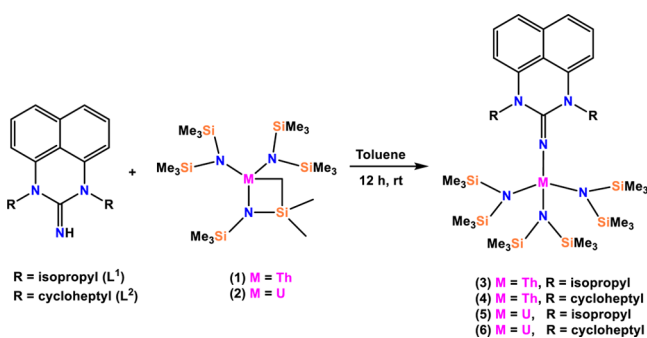
mentioned alterations would be achieved on a single ligand scaffold (Scheme 1 - bottom).

These structural adaptations influence the donor properties of the imine nitrogen as well as impose geometric constraints on the N-substituents compared to well-known imidazolin-2-imine motifs.

In the present study, we introduce new highly electron-rich six-membered N-heterocyclic iminato ligands (perimidin-2-iminato) and demonstrate their general synthesis containing alkyl N-substituents. The synthesis of the corresponding actinide(IV) complexes and their detailed structural examination bearing the perimidin-2-iminato moiety, as well as their applications toward the challenging addition of alcohol to diisopropylcarbodiimide (DIC) and 1,3-di-*p*-tolylcarbodiimide (DTC) to form the corresponding isoureas from moderate to excellent yields, under mild reaction condition, and short reaction times, are addressed. The presented study presents the scope of substrates, the effect of ancillary ligands, kinetics and thermodynamics studies of this challenging insertion reaction. To the best of our knowledge, this is the first disclosure of any organometallic complex containing the six-membered N-heterocyclic iminato system.

The synthesis of actinide(IV) complexes 3–6 was accomplished by a one-pot reaction between the actinide metallacycles 1 or 2 with 1 equiv of respective perimidin-2-imine at room temperature in toluene (Scheme 2). The reaction mixture was stirred for 12 h, and recrystallization from concentrated toluene solutions at $-35\text{ }^{\circ}\text{C}$ afforded X-ray quality crystals. The molecular structures of $[(L^1)\text{An}\{\text{N}(\text{SiMe}_3)_2\}_3]$ and $[(L^2)\text{An}\{\text{N}(\text{SiMe}_3)_2\}_3]$ (where $L^1 = (1,3\text{-diisopropyl-1H-perimidine-2(3H)-imine})$, $L^2 = (1,3\text{-dicycloheptyl-1H-perimidine-2(3H)-imine})$, and $\text{An} = \text{Th, U}$) were determined by X-ray diffraction.

Scheme 2. Synthesis of Mono(perimidin-2-iminato) Actinide(IV) Complexes 3–6



The selected bond distances and angles of complexes 3–6 are presented in Table 1.

Table 1. Selected Bond Lengths (Å) and Angles (deg) for Complexes 3–6

	complex 3	complex 4	complex 5	complex 6
An–N1	2.190(5)	2.225(7)	2.128(4)	2.156(7)
An–N4	2.380(4)	2.335(6)	2.308(4)	2.287(6)
An–N5	2.370(5)	2.312(5)	2.313(4)	2.328(7)
An–N6	2.361(5)	2.385(6)	2.294(4)	2.280(6)
N1–C1	1.289(7)	1.288(11)	1.295(6)	1.294(12)
An–N1–C1	162.7(4)	156.1(5)	163.4(4)	157.6(6)
N1–An–N4	108.51(16)	94.5(2)	109.91(15)	93.4(2)
N1–An–N5	96.38(16)	121.0(2)	95.68(15)	124.6(2)
N1–An–N6	103.61(16)	104.8(3)	102.67(14)	103.9(3)
N4–An–N5	118.56(15)	114.1(2)	119.76(14)	113.9(2)
N4–An–N6	108.25(15)	117.8(2)	107.78(14)	116.8(2)
N5–An–N6	119.16(16)	104.9(2)	118.60(13)	104.6(3)
cone angle	113.2	124.4	114.0	123.5

The mono(perimidin-2-iminato) Th(IV) complexes (3 and 4) were isolated as white crystalline compounds in high yields. The solid state structures of 3 and 4 are depicted in Figure 1a, b, respectively.

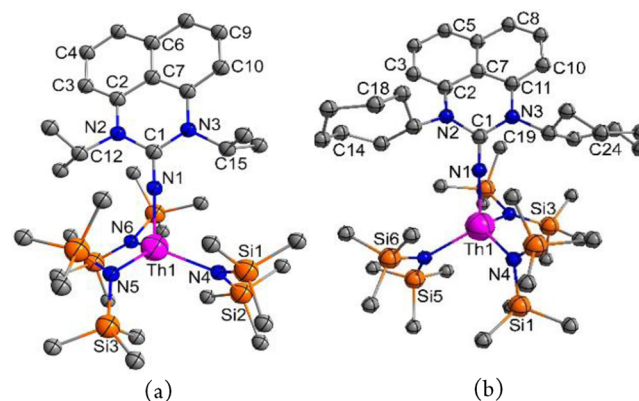


Figure 1. Molecular structure of complexes 3 (a) and 4 (b), with thermal ellipsoids set at the 50% probability levels. All hydrogen atoms are omitted for the clarity.

The X-ray structural analysis revealed that the central Th(IV) is in a distorted tetrahedral geometry consisting of one perimidin-2-iminato ligand and three N-silylated amido ($\text{N}\{\text{Si}(\text{CH}_3)_2\}_2$) groups. The perimidin-2-iminato ligand binds with the metal in a monodentate fashion, and the remaining three positions are occupied by amido ligands, completing the tetrahedral environment. The N1–C1_{ipso} bond distances are 1.289(7) and 1.288(11) Å for complexes 3 and 4, respectively, which are analogous to the corresponding bond lengths in related imidazolin-2-iminato complexes.^{8c} The Th–N1 bond distances in complexes 3 and 4 are 2.190(5) and 2.225(7) Å, respectively, which are found to be on average 0.19 Å shorter than the Th–N_{amido} bond length in complex 3 and 0.12 Å shorter in complex 4. The small bent Th–N1–C1 angles 162.7(4)° and 156.1(5)° for complexes 3 and 4, respectively, allow a substantial π donation from the ligand to the metal, indicating a double bond between the metal and the imine nitrogen.

The mono(perimidin-2-iminato) U(IV) complexes were isolated as brown crystalline compounds also in very high yields. The molecular structure of the $[(L^1)U\{N(SiMe_3)_2\}_3]$ (**5**) and $[(L^2)U\{N(SiMe_3)_2\}_3]$ (**6**) is depicted in Figure 2a,b,

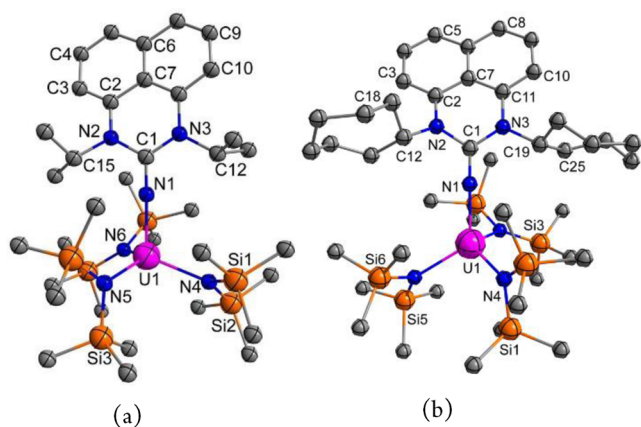


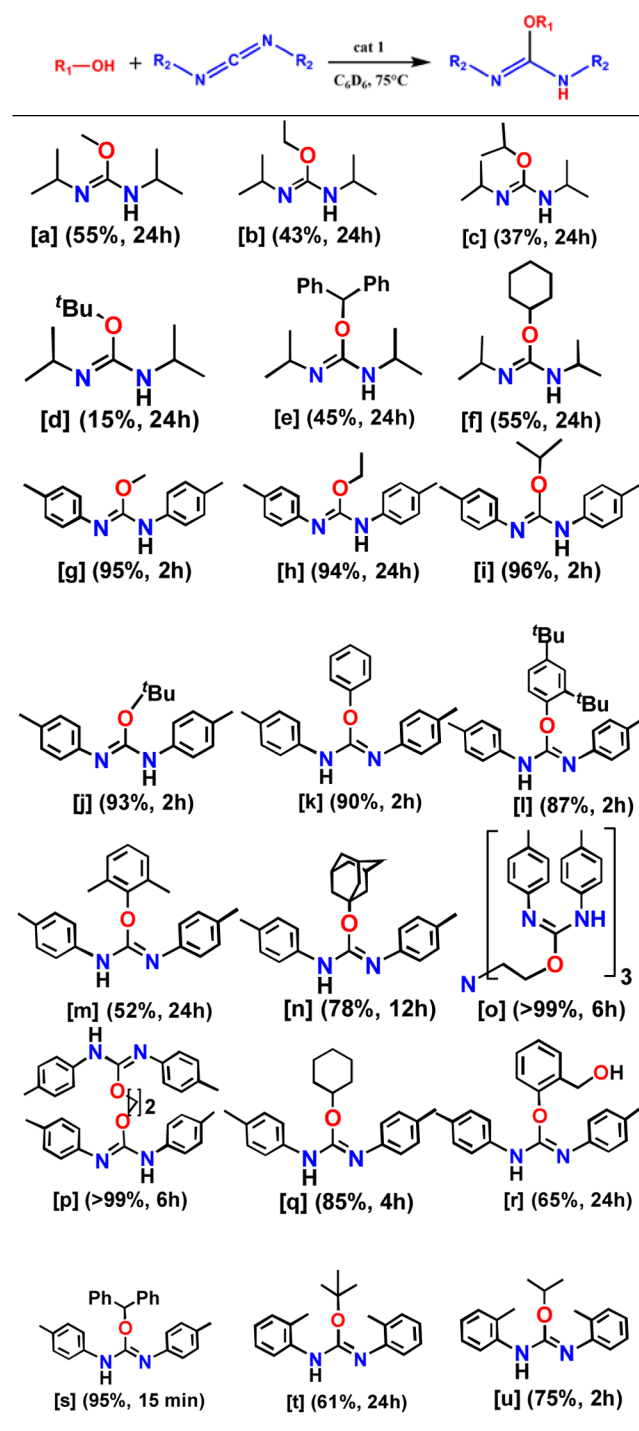
Figure 2. Molecular structure of complexes **5** (a) and **6** (b), with thermal ellipsoids set at the 50% probability levels. All hydrogen atoms are omitted for the clarity.

respectively. The distorted tetrahedral coordination environment around the central metal atom is approximately equivalent to that of its Th(IV) analogue. The U1–N1–C1 angles also depart from linearity and exhibit values of 163.4(4)° and 157.6(6)° for complexes **5** and **6**, respectively. Marginally shorter U–N1 bond lengths are observed as expected in comparison to the corresponding Th–N1 distances, displaying the values of 2.128(4) and 2.156(7) Å for compounds **5** and **6**, respectively. The short U–N1 bond lengths and the large U–N1–C1 angles indicate a significant π -character of the U–N1 bond, comparable to the respective Th–N1 bond (*vide supra*). The N1–C_{ipso} bond lengths in the mono(perimidin-2-iminato) uranium complexes **5–6** are almost identical to those in the thorium analogues, indicating that the bonding of the ligand to the metal can be described as a metalla-heterocumulene (An=N=C). Unexpectedly, as compared to the corresponding imidazolin-2-iminato thorium and uranium complexes, almost identical metal–amido and metal–imido bond distances are observed, with the only difference being the proximity of the N-alkyl substituents to the metal center.

In order to quantify the proximity of the wingtip substitutions to the coordinated metal, cone angles were measured for the present systems (113.2°, 124.4°, 114.0°, and 123.5° for complexes **3**, **4**, **5**, and **6**, respectively). These values are much smaller than in the analogous complex $[(Im^R N)An\{(N(SiMe_3)_2)_3\}]$ (where R = Dipp), which exhibits cone angle values 210° and 212° for Th and U, respectively. The smaller cone angle of the present systems implies significantly greater space available for the incoming substances to approach the metal center.

Encouraged by these observations, we investigate the challenging addition of alcohols to carbodiimides. In order to determine the catalyst with the highest possible efficiency, our initial exploratory findings showed that all complexes (**3–6**) are potentially capable to catalyze the addition of alcohols to carbodiimides, and all of them exhibit comparable activities (Table S2). The catalytic reaction of ^tBuOH with DTC is particularly impressive as it produces the corresponding isourea in excellent yield in short reaction time. For example, this

Table 2. Complex **3** Catalyzed Insertion of Alcohols to Carbodiimides^a



^aReaction conditions: 4 mg of catalyst (0.004 mmol, ~0.4 mol %); cat./alcohol: 1/100; cat./carbodiimide: 1/100; 550 μ L of C₆D₆; 75 °C; yield was determined by ¹H NMR spectroscopy of the crude reaction mixture.

particular substrates combination generated 93%, 86%, 89%, and 86% of the isourea catalyzed by complexes **3**, **4**, **5**, and **6**, respectively, within 2 h. It is important to point out that the ligand itself does not catalyze the reaction and freshly recrystallized complexes were used to run the catalytic reactions. Hence, further catalytic studies were carried out with complex **3**. The increasing trends of reactivity observed

from the aryl substituted carbodiimide (DTC) as compared to the alkyl substituted carbodiimide (DIC) are attributed to the higher electrophilic character (sp hybridized carbon) of DTC.

The composite effect of acidity and steric congestion of the alcohol played a crucial role in determining the product formation. With the increase of the steric hindrance from methanol to ^tBuOH, the amount of product formation with DIC markedly dropped significantly (entries [a]–[d], Table 2). Complex 3 was found to be superior considering our previous report, which showed no catalytic turnover in the DIC-^tBuOH substrate combination.¹⁶ The combination of DIC and 1-adamantanol did not lead to the product formation presumably to the steric congestion imposed by the adamantyl group. Sterically less crowded alcohols, *viz.*, diphenylmethanol and cyclohexanol, afforded higher conversion compared to ^tBuOH (entries [e] and [f], Table 2). However, the reaction of highly acidic phenol with DIC (not DTC) can be performed without a catalyst. The combination of DTC and alcohols (entries [g]–[s], Table 2) afforded excellent yields (80–99%) in 2 h. Identical trends as presented above are operative for DTC, when the amount of the product decreases with an increase of the steric encumbrance of the alcohol (entries [k]–[m], Table 2).

Di- and trihydroxy substrates provided almost quantitative formation of the corresponding di- and tri-substituted isoureas in 6 h (entries [o]–[p], Table 2). In order to determine the competing reactivity of aliphatic and aromatic alcohols, the insertion reaction was attempted with salicylic alcohol (entry [r], Table 2). The aromatic alcohol selectively inserts into DTC, which can be attributed to its higher acidity as compared to its aliphatic analogue.

Diphenylmethanol was found to be extremely reactive, and 95% product formation was obtained within 15 min (entry [s], Table 2). In order to investigate the effect of the substituents present in the phenyl group of DTC, we carried out the reaction with di-*o*-tolylcarbodiimide (*o*-DTC) and ^tBuOH or isopropanol. In both cases, *o*-DTC gave lower yields (entries [t] and [u], Table 2) as compared to its *para* analogue (DTC), presumably due to its steric effects.

In order to gain an insight into the reaction mechanism, stoichiometric reactions of complex 3 with 2,4-di-*tert*-butylphenol (^tBu₂PhOH) and DTC were carried out independently. The addition of stoichiometric amounts or even an excess of DTC to complex 3 did not lead to the displacement of the coordinating iminato ligand to form the corresponding guanidinate species, suggesting the retention of the ligand coordinated to the metal during the catalytic cycle. The addition of 3 equiv of alcohol led to dislodgement of 1 equiv of [HN(SiMe₃)₂] in 15 min and complete replacement of the other two amido bonds up to 45 min (Figure S9), without affecting the iminato ligand coordination, indicating that the tris-alkoxo species [(Pr^RN)An(OR)₃] (I) can be proposed as an operative active intermediate for the reaction.

The initial rate of reaction was measured to determine the order of the substrates and catalyst. Reactions were performed with variable concentrations of catalyst, ^tBu₂PhOH, and DTC, while keeping the other reagents concentration unchanged. The initial rate of the reaction varies linearly with the slope, revealing that the reactions displayed first-order dependence on DTC (Figure 3), ^tBu₂PhOH (Figure 4) and as well as on complex 3 (Figure 5), giving rise to the kinetic rate eq 1.

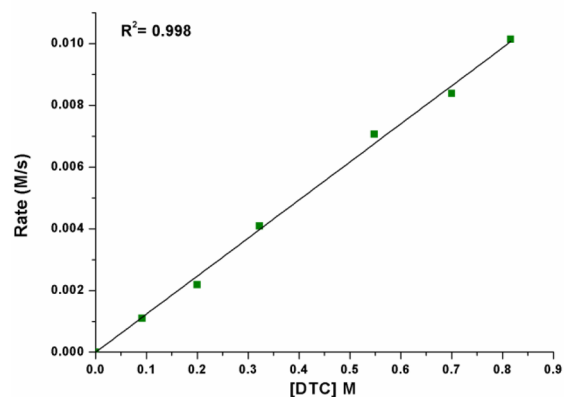


Figure 3. Plot of the initial reaction rate as a function of DTC concentration in the reaction of ^tBu₂PhOH with DTC.

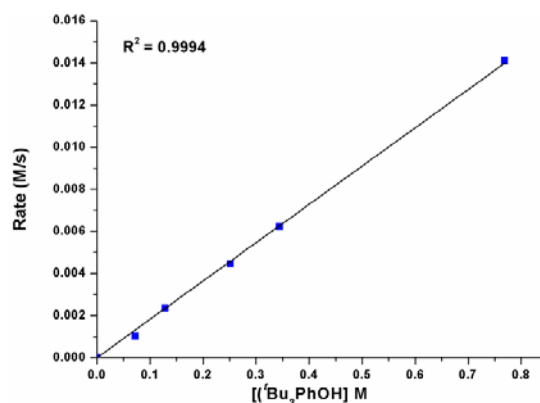


Figure 4. Plot of the initial reaction rate as a function of ^tBu₂PhOH concentration in the reaction of ^tBu₂PhOH with DTC.

$$\frac{dp}{dt} = k_{\text{obs}} \times [\text{DTC}]^1 \times [{}^t\text{Bu}_2\text{PhOH}]^1 \times [3]^1 \quad (1)$$

Equation 1: Kinetic rate equation of the insertion of ^tBu₂PhOH to DTC.

In addition, the kinetic isotope effect was studied by performing the reaction with the deuterated alcohol (^tBu₂PhOD), resulting in a KIE value of 1.74, indicating that the protonolysis step is the turn over limiting step (Scheme 3).¹⁸

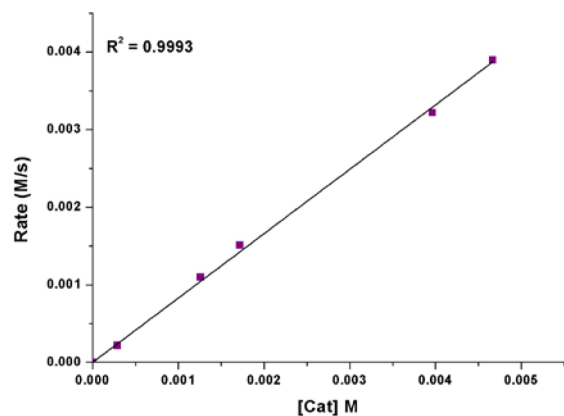
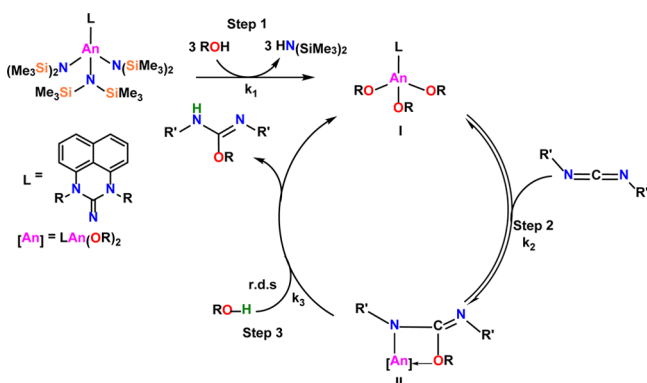


Figure 5. Plot of reaction rate as a function of complex 3 concentration in the reaction of ^tBu₂PhOH with DTC.

Scheme 3. Plausible Mechanism of the Actinide-Mediated Catalytic Insertion of Alcohol into Carbodiimide



The activation parameters were determined from the Eyring (Figure 6) and Arrhenius plots, with ΔH^\ddagger , ΔS^\ddagger , and E_a values

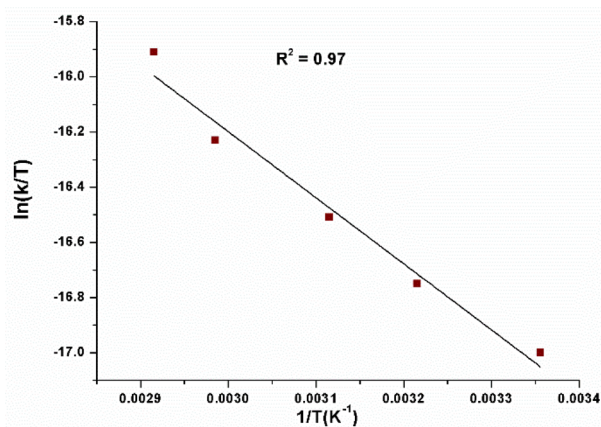


Figure 6. Eyring plot of $t\text{Bu}_2\text{PhOH}$ addition to DTC mediated by complex 3.

of $4.8 \pm 0.4 \text{ kcal mol}^{-1}$, $-51.48 \pm 0.4 \text{ e.u.}$, and $5.3 \pm 0.4 \text{ kcal mol}^{-1}$, respectively. The large negative entropy value corroborates a highly ordered transition state at the rate-determining step.¹⁸ On the basis of the kinetics and the thermodynamic parameters in combination with the stoichiometric reactions, a plausible mechanism is presented in Scheme 3.

The first step of the proposed mechanism is the rapid protonolysis of the starting actinide complex 3 by the alcohol with the displacement of 3 equiv of hexamethyldisilazane producing complex I. This process is thermodynamically favorable due to the oxophilic nature of the thorium ($\Delta H_{\text{calcd}} = -68 \text{ kcal/mol}$).¹⁹ Migratory insertion of DTC to the corresponding Th–O is in a rapid equilibrium (step 2), producing complex II that follows a protonolytic cleavage (RDS) with another equivalent of an alcohol (step 3), yielding the isourea product and regenerating the active catalyst I. Interestingly, starting the catalytic reaction with the trisalkoxo complex I was found to yield similar results as compared with when the reaction was performed with complex 3. For example, in the reaction of $t\text{Bu}_2\text{PhOH}$ with DTC, 80% yield of the corresponding isourea was obtained after 2 h (Figure S11) as compared to 87% using complex 3 (entry [j] in Table 2).

To trap the migratory inserted intermediate II of the catalytic cycle shown in Scheme 3, 1 equiv of DTC was reacted with 1

equiv of complex I, and the intermediate was characterized by $^1\text{H NMR}$ (Figure 7). We decided to perform the reaction with

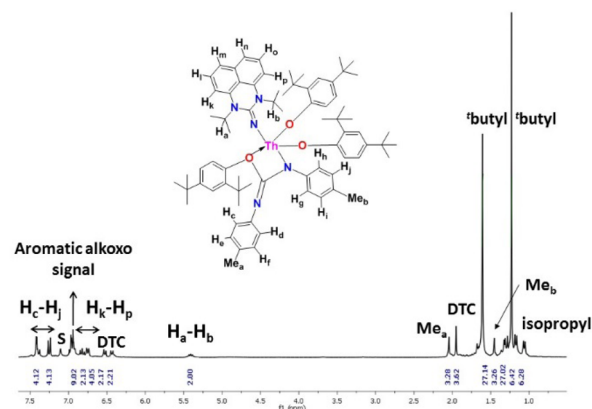


Figure 7. NMR spectrum of complex II (S = solvent).

1 equiv of DTC to avoid overlapping signals when more equivalents of DTC insert into the additional alkoxy moieties. In addition, theoretically there are two fashions in which we can depict the migratory inserted complex II: One in which the two nitrogen atoms of the inserted DTC are attached to the metal or a complex in which one nitrogen and one oxygen atom are attached to the metal as shown in Scheme 3 and corroborated by the NMR of this complex.

CONCLUSION

Here, we disclose for the first time the synthesis of a new family of six-membered N-heterocyclic iminato ligands and their incorporation with actinides to obtain active catalysts for the insertion of primary, secondary, tertiary, and aromatic alcohols into carbodiimides, affording the corresponding isoureas. Diol and triol substrates were also found to be highly active, producing the corresponding bis- and tris-isoureas, in quantitative yields. The intermediate complexes I and II were trapped spectroscopically. Here, we have shown that the steric effects of the perimidin-2-iminato moiety, as opposed to the electronic effects, are the major operative factor for the product formation, as compared to the imidazolin-2-iminato moiety in actinide complexes.

EXPERIMENTAL SECTION

All manipulations of air-sensitive materials were performed with the rigorous exclusion of oxygen and moisture in flamed Schlenk-type glassware or J-Young Teflon valve-sealed NMR tubes on a dual manifold Schlenk line interfaced to a high vacuum (10^{-5} Torr) line, or in a nitrogen-filled Innovative Technologies glovebox with a medium-capacity recirculator (1–2 ppm of O_2). Argon and nitrogen were purified by passage through a MnO oxygen-removal column and a Davison 4 Å molecular sieve column. Hydrocarbon solvents benzene- d_6 (Cambridge Isotopes), toluene (Bio-Lab), and diethyl ether (Bio-Lab) were distilled under vacuum from Na/K alloy. 1,3-Diisopropylcarbodiimide was distilled from sodium bicarbonate under a nitrogen atmosphere, and 1,3-di-*p*-tolylcarbodiimide was dried under vacuum (10^{-6}) for 12 h on a high vacuum line. Methanol and ethanol were dried using sodium (Na) metal, distilled, and stored over 4 Å molecular sieves. Isopropanol and *tert*-butanol were refluxed over CaH_2 , distilled, and stored over 4 Å molecular sieves. The actinide complexes $[(\text{Me}_3\text{Si})_2\text{N}]_2\text{An}[\kappa^2\text{-(N,C)CH}_2\text{Si(CH}_3)_2\text{N(SiMe}_3)]$ (An = Th (1), U (2)),²⁰ N^1, N^8 -diisopropyl-naphthalene-1,8-diamine, and N^1, N^8 -dicycloheptyl-naphthalene-1,8-diamine were prepared according

to published procedures.²¹ All the aforementioned reagents were stored in an inert atmosphere glovebox prior to use.

NMR spectra were recorded on Bruker Avance 300, Bruker Avance III 400 spectrometers. Chemical shifts for ¹H and ¹³C NMR are referenced to internal protio solvent and reported relative to tetramethylsilane. *J*-values are reported for ¹H NMR coupling constants in the unit of hertz (Hz).

The single-crystal material was immersed in perfluoropolyalkylether and was quickly fished with a glass rod and mounted on a Kappa CCD diffractometer under a cold stream of nitrogen. Data collection was performed using monochromated Mo K α radiation using φ and ω scans to cover the Ewald sphere.²² Accurate cell parameters were obtained with the amount of indicated reflections.²³ The structure was solved by SHELXS-97 direct methods²⁴ and refined by the SHELXL-97 program package.²⁵ The atoms were refined anisotropically. Hydrogen atoms were included using the riding model. Figures were drawn (50% probability thermal ellipsoids) using Diamond V3.1.²⁶

Synthesis of L¹-HBr (2-Amino-1,3-diisopropyl-1H-perimidinium Bromide). A solution of cyanogen bromide (0.61 g, 5.76 mmol) in toluene (20 mL) was added dropwise to a stirred solution of diamine *N,N'*-diisopropyl-1,8-diaminonaphthalene (1.1634 g, 4.8 mmol) in toluene at 110 °C. A dark solid started to precipitate during the course of the addition. After complete addition, the mixture was stirred at 110 °C for 12 h. The mixture was allowed to cool to room temperature, and the precipitate was filtrated, followed by washed with diethyl ether (3 \times 30 mL) and dried in vacuum, to afford a dark solid. Yield: 1.55 g (93%). ¹H NMR (400 MHz, CDCl₃): δ = 8.35 (s, 2H, NH₂), 7.50–7.38 (m, 4H, ArCH), 7.10 (d, *J* = 8.0 Hz, 2H), 5.06 (m, 2H), 1.70 (d, *J* = 6.0 Hz, 12H); ¹³C NMR (100 MHz, CDCl₃): δ = 153.0 (NCN), 133.8 (ArC), 132.2 (ArC), 129.1 (ArC), 128.4 (ArC), 127.0 (ArC), 125.2 (ArC), 123.1 (Ar C), 110.4 (ArC), 55.4 (CHMe₂), 21.2 (CH₃) ppm. ESI-MS, *m/z*: 348.0889, Anal. Calcd for C₁₈H₂₁N₃Br: C, 60.17; H, 5.89; N, 11.70. Found: C, 60.80; H, 5.92; N, 11.79.

Synthesis of L²-HBr (2-Amino-1,3-dicycloheptyl-1H-perimidinium Bromide). This was synthesized following the similar procedure described for the synthesis of L¹-HBr by reaction between cyanogen bromide (0.9 g, 5.66 mmol) and *N,N'*-diisopropyl-1,8-diaminonaphthalene. The resulting precipitate was washed with diethyl ether (3 \times 30 mL) and dried in vacuum to afford an off-white solid. Yield: 1.1 g (94%). ¹H NMR (400 MHz, CDCl₃): δ = 7.93 (s, 2H, NH₂), 7.47–7.37 (m, 4H, ArCH), 6.97 (d, 2H, *J* = 8.0 Hz, ArCH), 4.67–4.57 (m, 2H), 2.43–2.32 (m, 4H, CH₂), 2.18–2.08 (m, 4H, CH₂), 1.80–1.70 (m, 12H, CH₂), 1.63–1.57 (m, 4H, CH₂); ¹³C NMR (75.5 MHz, CDCl₃): δ = 151.0 (NCN), 133.8 (ArC), 127.6 (ArC), 122.9 (ArC), 120.6 (ArC), 110.5 (ArC), 64.8, 31.8, 27.8, 26.4 ppm; Anal. Calcd for C₂₅H₃₄N₃Br: C, 65.78; H, 7.51; N, 9.21. Found: C, 65.87; H, 7.57; N, 9.29.

Synthesis of L¹ (1,3-Diisopropyl-1H-perimidine-2(3H)-imine). Aqueous KOH (1.00 g, 17.82 mmol) was added to the diethyl ether (40 mL) suspension of L¹-HBr (2.50 g, 7.18 mmol), and the mixture was vigorously stirred for 30 min at ambient temperature. In a separatory funnel, the two layers were separated and the aqueous layer was extracted with diethyl ether (3 \times 30 mL). The combined organic phases were dried over anhydrous Na₂SO₄. After filtration, the solvent was removed in vacuo to afford an off-white solid. Yield: 1.75 g (92%). ¹H NMR (400 MHz, CDCl₃): δ = 7.24–7.19 (m, 2H, ArCH), 7.12 (d, *J* = 8.0 Hz, ArCH, 1H), 6.66 (d, *J* = 8.0 Hz, ArCH, 2H), 4.93 (br, 2H, CHMe₂), 1.52 (d, 12H, CHMe₂); ¹³C NMR (100 MHz, CDCl₃): δ = 151.6 (NCN), 137.4 (ArC), 134.4 (ArC), 127.2 (ArC), 118.1 (ArC), 116.5 (ArC), 105.2 (ArC), 49.6 (CHMe₂), 19.6 (CH₃) ppm. ESI-MS, *m/z*: 268.1827, Anal. Calcd for C₁₈H₂₀N₃: C, 77.66; H, 7.24; N, 15.09. Found: C, 77.58; H, 7.31; N, 15.15.

Synthesis of L² (1,3-Dicycloheptyl-1H-perimidine-2(3H)-imine). This was synthesized following the similar procedure described for the synthesis of L¹ by reaction between L²-HBr (0.8 g, 5.66 mmol) and aqueous KOH in diethyl ether. The aqueous layer was extracted with diethyl ether (3 \times 30 mL). The combined organic phases were dried over anhydrous Na₂SO₄. After filtration, the solvent was removed under vacuo to afford a light brown solid. Yield: 0.6 g

(92%). ¹H NMR (400 MHz, CDCl₃): δ = 7.22–7.18 (m, 2H, Ar-CH), 7.09 (d, 2H, *J* = 6.0 Hz, ArCH), 6.59 (d, 2H, *J* = 6.0 Hz, ArCH), 4.58–4.46 (m, 2H, CH_{cycloheptyl}), 2.38–2.28 (m, 4H, CH₂), 1.89–1.79 (m, 4H, CH₂), 1.79–1.70 (m, 4H, CH₂), 160–1.51 (m, 12H, CH₂); ¹³C NMR (100 MHz, CDCl₃): δ = 150.6 (NCN), 134.3 (ArC), 127.2 (ArC), 118.5 (ArC), 116.5 (ArC), 64.7, 31.3, 28.7, 27.0 ppm. Calcd for C₂₅H₃₃N₃: C, 79.95; H, 8.86; N, 11.19. Found: C, 79.88; H, 8.81; N, 11.12.

General Procedure for the Synthesis of Mono(perimidin-2-iminato) Actinide (IV) Complexes. A toluene (10 mL) solution of actinide metallacycle **1** or **2** (200 mg) was reacted with the respective perimidin-2-imine (1 equiv in 10 mL) at room temperature, and the reaction was stirred for an additional 12 h at room temperature. The solvent was removed under reduced pressure to afford the crude solid **3–6**. X-ray quality crystals were grown from concentrated toluene solution at –35 °C.

[(L¹)Th{N(SiMe₃)₂}₃] (3). Yield 94% (260 mg, 0.265 mmol); ¹H NMR (300.0 MHz, C₆D₆): δ = 7.16–7.12 (m, 4H, ArCH), 6.81–6.78 (m, 2H, ArCH), 5.93–5.83 (m, 2H, CHMe₂), 1.52 (d, *J* = 8.0 Hz, 12H, CHMe₂), 0.45 (s, 54H, Si(CH₃)₃); ¹³C NMR (75.5 MHz, C₆D₆): δ = 143.1 (C_{ipso=N}), 135.8 (ArC), 135.1 (ArC), 129.0 (ArC), 126.4 (ArC), 118.7 (ArC), 117.4 (ArC), 106.0 (ArC), 49.7 (CHMe₂), 19.7 (CH₃), 4.75 (Si(CH₃)₃) ppm. Calcd for C₃₅H₇₄N₆Si₆Th: C, 42.91; H, 7.61; N, 8.58. Found: C, 42.98; H, 7.67; N, 8.65.

[(L²)Th{N(SiMe₃)₂}₃] (4). Yield 92% (280 mg, 0.257 mmol); ¹H NMR (300.0 MHz, C₆D₆): δ = 7.22–7.11 (m, 4H, ArCH), 6.83–6.80 (m, 2H, ArCH), 5.39–5.28 (m, 2H, CH), 2.39–2.28 (m, 2H, CH₂), 2.01–1.92 (m, 2H, CH₂), 1.69–1.57 (m, 6H, CH₂), 1.46–1.37 (m, 2H, CH₂), 0.45 (s, 54H, Si(CH₃)₃); ¹³C NMR (75.5 MHz, C₆D₆): δ = 144.5 (C_{ipso=N}), 136.7 (ArC), 134.9 (ArC), 126.3 (ArC), 118.6 (ArC), 118.7 (ArC), 107.9 (ArC), 59.7 (ArC), 31.5 (CH₂), 29.4 (CH₂), 26.3 (CH₂), 5.26 (Si(CH₃)₃) ppm. Calcd for C₄₃H₈₆N₆Si₆Th: C, 47.48; H, 7.96; N, 7.72. Found: C, 47.54; H, 8.01; N, 7.79.

[(L¹)U{N(SiMe₃)₂}₃] (5). Yield 93% (255 mg, 0.258 mmol); ¹H NMR (300.0 MHz, C₆D₆, 298 K): δ = 13.02 (br, 12H, CHMe₂), 11.52–11.22 (m, 4H, ArCH), 7.28–6.99 (m, 2H, ArCH), 0.22–0.06 (m, 2H, CHMe₂), –11.48 (s, 54H, Si(CH₃)₃); ¹³C NMR (75.5 MHz, C₆D₆, 298 K): δ = 168.86 (C_{ipso=N}), 146.03 (ArC), 135.29 (ArC), 126.39 (ArC), 122.89 (ArC), 118.69 (ArC), 48.07 (CHMe₂), 20.30 (CH₃), 2.13 (Si(CH₃)₃) ppm. C₃₅H₇₄N₆Si₆U: C, 42.65; H, 7.57; N, 8.53. Found: C, 42.71; H, 7.61; N, 8.59.

[(L²)U{N(SiMe₃)₂}₃] (6). Yield 90% (275 mg, 0.251 mmol); ¹H NMR (300.0 MHz, C₆D₆, 298 K): δ = 19.0 (br, 3H, CH_{cycloheptyl}), 14.9 (br, s, 2H, ArCH), 14.3 (br, s, 2H, CH_{cycloheptyl}), 11.1 (m, 2H, ArCH), 11.0 (m, 2H, ArCH), 4.95 (br, s, 4H, CH_{cycloheptyl}), 3.55 (br, s, 9H, CH_{cycloheptyl}), –12.33 (s, 54H, Si(CH₃)₃); ¹³C NMR (75.5 MHz, C₆D₆, 298 K): δ = 169.1 (C_{ipso=N}), 135.8 (ArC), 143.5 (ArC), 134.0 (ArC), 130.0 (Ar C), 123.9 (ArC), 121.0 (ArC), 42.0 (CH_{cycloheptyl}), 31.4 (CH_{2cycloheptyl}), 30.7 (CH_{cycloheptyl}), 5.51 (Si(CH₃)₃) ppm. Calcd for C₄₃H₈₆N₆Si₆U: C, 47.22; H, 7.92; N, 7.68. Found: C, 47.30; H, 7.98; N, 7.73.

General Procedure for the Catalytic Addition of Alcohols to Carbodiimides. In a typical experiment, approximately 4 mg of the desired catalyst in 600 μ L of C₆D₆ was transferred to a J-Young Teflon sealed NMR tube, followed by the addition of carbodiimide (100 equiv) and alcohol (100 equiv). Samples were then placed in an oil bath preheated to 75 °C, and the reaction progress was monitored at regular intervals using ¹H NMR spectroscopy for up to 24 h. After completion of the reaction, crude mixtures were analyzed using ¹H, ¹³C spectroscopy as well as mass spectrometry. Known compounds were compared to those previously reported in the literature.

■ ASSOCIATED CONTENT

Supporting Information

The Supporting Information is available free of charge on the ACS Publications website at DOI: 10.1021/acs.organomet.7b00037.

Schematic synthesis of L¹ and L²; characterization of isoureas; characterization of L¹-HBr, L²-HBr, L¹, L², and

complexes 3–6; catalytic addition of alcohols to carbodiimides mediated by complexes 3–6 as a function of time; stoichiometric reaction of complex 3 and ^tBu₂PhOH; stoichiometric reaction of complex 3, ^tBu₂PhOH, and DTC; and crystallographic table (PDF) Crystallographic data for 5 (CIF) Crystallographic data for 6 (CIF) Crystallographic data for 3 (CIF) Crystallographic data for 4 (CIF)

AUTHOR INFORMATION

Corresponding Author

*E-mail: chmoris@tx.technion.ac.il.

ORCID

Moris S. Eisen: 0000-0001-8915-0256

Notes

The authors declare no competing financial interest.

ACKNOWLEDGMENTS

This work was supported by the Israel Science Foundation administered by the Israel Academy of Science and Humanities under Contract No. 78/14; and by the PAZY Foundation Fund (2015) administered by the Israel Atomic Energy Commission.

REFERENCES

- (1) (a) Barnea, E.; Eisen, M. S. *Coord. Chem. Rev.* **2006**, *250*, 855–899. (b) Andrea, T.; Eisen, M. S. *Chem. Soc. Rev.* **2008**, *37*, 550–567. (c) Evans, W. J.; Kozimor, S. A.; Ziller, J. W. *Science* **2005**, *309*, 1835–1838. (d) Summerscales, O. T.; Cloke, F. G. N.; Hitchcock, P. B.; Green, J. C.; Hazari, N. *Science* **2006**, *311*, 829–831. (e) Hayton, T. W.; Boncella, J. M.; Scott, B. L.; Palmer, P. D.; Batista, E. R.; Hay, P. J. *Science* **2005**, *310*, 1941–1943. (f) Burns, C. J.; Eisen, M. S. Homogeneous and Heterogeneous Catalytic Processes Promoted by Organoactinides. In *The Chemistry of the Actinide and Transactinide Elements*, 3rd ed.; Morss, L. R., Edelstein, N., Fuger, J., Eds.; Springer: Dordrecht, Netherlands, 2006; pp 2911–3012.
- (2) (a) Bruno, J. W.; Smith, G. M.; Marks, T. J.; Fair, C. Kay.; Schultz, A. J.; Williams, J. M. *J. Am. Chem. Soc.* **1986**, *108*, 40–56. (b) Smith, G. M.; Carpenter, J. D.; Marks, T. J. *J. Am. Chem. Soc.* **1986**, *108*, 6805–6807. (c) Chen, Y. X.; Metz, M. V.; Li, L.; Stern, C. L.; Marks, T. J. *J. Am. Chem. Soc.* **1998**, *120*, 6287–6305. (d) Gillespie, R. D.; Burwell, R. L., Jr.; Marks, T. J. *Langmuir* **1990**, *6*, 1465–1477.
- (3) (a) Straub, T.; Haskel, A.; Neyroud, T. G.; Kapon, M.; Botoshansky, M.; Eisen, M. S. *Organometallics* **2001**, *20*, 5017–5035. (b) Hayes, C. E.; Platel, R. H.; Schafer, L. L.; Leznoff, D. B. *Organometallics* **2012**, *31*, 6732–6740. (d) Karmel, I. S. R.; Batrice, R. J.; Eisen, M. S. *Inorganics* **2015**, *3*, 392–428. (e) Wang, D.; van Gunsteren, W. F.; Chai, Z. *Chem. Soc. Rev.* **2012**, *41*, 5836–5865. (e1) Tobisch, S. *Chem. - Eur. J.* **2010**, *16*, 3441–3458. (f) Stubbert, B. D.; Marks, T. J. *J. Am. Chem. Soc.* **2007**, *129*, 6149–6167. (g) Stubbert, B. D.; Marks, T. J. *J. Am. Chem. Soc.* **2007**, *129*, 4253–4371. (h) Stubbert, B. D.; Stern, C. L.; Marks, T. J. *Organometallics* **2003**, *22*, 4836–4838. (i) Haskel, A.; Straub, T.; Eisen, M. S. *Organometallics* **1996**, *15*, 3773–3775.
- (4) (a) Wobser, S. D.; Marks, T. J. *Organometallics* **2013**, *32*, 2517–2528. (b) Dondoni, A.; Marra, A. *Eur. J. Org. Chem.* **2014**, *2014*, 3955–3969. (c) Weiss, C. J.; Marks, T. J. *Dalton Trans.* **2010**, *39*, 6576–6588.
- (5) (a) Dash, A. K.; Wang, J. X.; Berthet, J. C.; Ephritikhine, M.; Eisen, M. S. *J. Organomet. Chem.* **2000**, *604*, 83–98. (b) Iglesias, M.; Fernández-Alvarez, F. J.; Oro, L. A. *ChemCatChem* **2014**, *6*, 2486–2489.
- (6) Zeng, X. *Chem. Rev.* **2013**, *113*, 6864–6900 and references therein.
- (7) Haynes, W. M., Ed. *CRC Handbook of Chemistry and Physics*, 96th ed.; CRC Press: Boca Raton, FL, 2015; pp 2015–2016.
- (8) (a) Sharma, M.; Andrea, T.; Brookes, N. J.; Yates, B. F.; Eisen, M. S. *J. Am. Chem. Soc.* **2011**, *133*, 1341–1356. (b) Andrea, T.; Barnea, E.; Eisen, M. S. *J. Am. Chem. Soc.* **2008**, *130*, 2454–2455. (c) Karmel, I. S. R.; Fridman, N.; Tamm, M.; Eisen, M. S. *J. Am. Chem. Soc.* **2014**, *136*, 17180–17192.
- (9) Karmel, S. R. I.; Fridman, N.; Tamm, M.; Eisen, M. S. *Organometallics* **2015**, *34*, 2933–2942.
- (10) Walshe, A.; Fang, J.; Maron, L.; Baker, R. J. *Inorg. Chem.* **2013**, *52*, 9077–9086.
- (11) Baker, R. J.; Walshe, A. *Chem. Commun.* **2012**, *48*, 985–987.
- (12) Zhang, W.-X.; Xu, L.; Xi, Z. *Chem. Commun.* **2015**, *51*, 254–265.
- (13) Zarate, S. G.; Santana, A. G.; Bastida, A.; Revuelta, J. *Curr. Org. Chem.* **2014**, *18*, 2711–2749.
- (14) Karmel, S. R. I.; Eisen, M. S.; Tamm, M. *Angew. Chem., Int. Ed.* **2015**, *54*, 12422–12425.
- (15) For a copper complex, see: Wang, M. F.; Golding, B. T.; Potter, G. A. *Synth. Commun.* **2000**, *30*, 4197–4204.
- (16) Batrice, R. J.; Kefalidis, C. E.; Maron, L.; Eisen, M. S. *J. Am. Chem. Soc.* **2016**, *138*, 2114–2117.
- (17) Wu, X.; Tamm, M. *Coord. Chem. Rev.* **2014**, *260*, 116–138.
- (18) Burns, C. J.; Eisen, M. *Organoactinide Chemistry: Synthesis and Characterization*. In *The Chemistry of the Actinide and Transactinide Elements*; Morss, L., Edelstein, N., Fuger, J., Eds.; Springer: Dordrecht, Netherlands, 2006; pp 2799–2910.
- (19) Simoes, J. A. M.; Beauchamp, J. L. *Chem. Rev.* **1990**, *90*, 629–688.
- (20) (a) Simpson, S. J.; Turner, H. W.; Andersen, R. A. *J. Am. Chem. Soc.* **1979**, *101*, 7728–7729. (b) Simpson, S. J.; Andersen, R. A. *J. Am. Chem. Soc.* **1981**, *103*, 4063–4066. (c) Simpson, S. J.; Turner, H. W.; Andersen, R. A. *Inorg. Chem.* **1981**, *20*, 2991–2995. (d) Cantat, T.; Scott, B. L.; Kiplinger, J. L. *Chem. Commun.* **2010**, *46*, 919–921.
- (21) Bazinet, P.; Ong, T. – G.; O'Brien, J. S.; Lavoie, N.; Bell, E.; Yap, G. P. A.; Korobkov, I.; Richeson, D. S. *Organometallics* **2007**, *26*, 2885–2895.
- (22) *Kappa CCD Server Software*; Nonius BV: Delft, The Netherlands, 1997.
- (23) Otwinowski, Z.; Minor, W. *Methods Enzymol.* **1997**, *276*, 307–326.
- (24) Sheldrick, G. M. *Acta Crystallogr., Sect. C: Struct. Chem.* **2015**, *71*, 3–8.
- (25) Farrugia, L. J. *J. Appl. Crystallogr.* **2012**, *45*, 849–854.
- (26) Brandenburg, K. *Diamond (Version 3.1e), Crystal and Molecular Structure Visualization*; Crystal Impact, K. Brandenburg & H. Putz Gbr: Bonn, Germany, 2007.